Derivation and Comparison of Efficiency and Power in Non-resonant and Resonant Circuit of Capacitive Power Transfer

Shunya Kuroda and Takehiro Imura

Faculty of Electronical Engineering, Tokyo University of Science

Abstract Capacitive Power Transfer (CPT) is safer than Inductive Power Transfer (IPT). In this study, conditions for transfer with high efficiency and high power were presented by deriving equation of the resonance conditions, efficiency, power, and optimum load considering internal resistance in non-resonance (N-N), secondary resonance (N-S), primary resonance (S-N) , electric resonant coupling (S-S) and (S-P) without approximation. In addition, the value of efficiency and power are derived and compared in the five topologies. As a result, it is said that S-S and S-P can transfer with high efficiency and high power and are superior to other topologies.

Keyword Capacitive Power Transfer, non-resonant circuit, resonant circuit, internal resistance, efficiency, power, optimum load, without approximation

1. INTRODUCTION

Wireless power transfer (WPT) announced by MIT in 2007, WPT is getting much global expectation as a way to solve the problem of cable charging. [1] Wireless power transfer in the short distance is divided into electric field coupling (CPT) and magnetic field coupling (IPT). The CPT needs only metal plates, so it is cheaper and lighter than IPT. In addition, CPT doesn't have risks of decreasing efficiency and rising temperature due to metallic foreign objects. Owing to these advantages, CPT will be able to use in various applications. Therefore, research of CPT has been prospered in recent years. [2-4] However, CPT is less researched than IPT.

In this paper, the resonance conditions, efficiency, optimum load, and output power are derived in five topologies of CPT circuit considering internal resistance.

Furthermore, five topologies are compared. The optimum load in this paper maximizes efficiency in the resonance condition.

2. BASIC STRUCTURE OF CAPACITIVE POWER TRANSFER

Figure 1 shows a CPT coupler with horizontal structure. Coupling part of CPT consists of four metal plates. The power supply side is called the power transmitter coupler, and the load side is called the power receiver coupler. Figure 2 shows the equivalent circuit of the power transmitter / receiver coupler. The self-capacitances C_1 , C_2 and the mutual capacitance C_m can be represented by from (1) to (3).

$$C_1 = C_{12} + \frac{(C_{13}+C_{14})(C_{23}+C_{24})}{C_{13}+C_{14}+C_{23}+C_{24}} \tag{1}$$

$$C_2 = C_{34} + \frac{(C_{13}+C_{14})(C_{23}+C_{24})}{C_{13}+C_{14}+C_{23}+C_{24}} \tag{2}$$

$$C_m = \frac{C_{24}C_{13}-C_{14}C_{23}}{C_{13}+C_{14}+C_{23}+C_{24}} \tag{3}$$

3. FAVE TOPOLOGIES OF CAPACITIVE POWER TRANSFER

There are five circuit topologies: non-resonance (N-N), secondary resonance (N-S), primary resonance (S-N), electric resonant coupling (S-S) and (S-P). Each topology is shown in Fig3 to Fig7. Efficiency η is represented by equation (4). P_{r1}, P_{r2} , and P_2 are expressed by equations from (5) to (7). P_{r1},P_{r2},and P_2 are the power consumptions at r_1, r_2, and R_L.

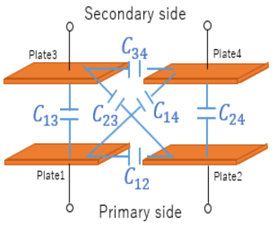

Fig 1 CPT coupler

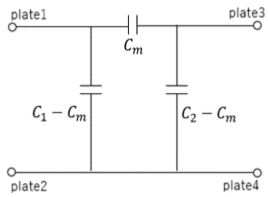

Fig 2 Equivalent circuit of CPT coupler

$$\eta = \frac{P_2}{P_{r1}+P_{r2}+P_2} \tag{4}$$

$$P_{r1} = r_1|I_1|^2 \tag{5}$$

$$P_{r_2} = r_2|I_2|^2 \tag{6}$$

$$P_2 = R_L|I_2|^2 \tag{7}$$

$P_{r2}$and P_2 of the (S-P) are represented by (8) and (9)

$$P_{r_2} = r_2\left|I_{r_2}\right|^2 \tag{8}$$

$$P_2 = R_L\left|I_{R_L}\right|^2 \tag{9}$$

4. DERIVATION OF THEORETICAL FORMULA

In this chapter, the resonance conditions, efficiency, output power, and optimum load in the five topologies are derived.

As an example, S-S is showed for the derivation process. Fig. 8 shows an equivalent circuit with S-S topology circuit shown in Fig. 6. In addition, each impedance is shown in equations from (10) to (12).

$$Z_{in2} = \frac{1}{\frac{1}{R_L+r_2+j\omega L_2}+j\omega C_2} \tag{10}$$

$$Z_2 = \frac{1}{\omega^2 C_m^2 Z_{in2}} \tag{11}$$

$$Z_{in1} = \frac{1}{j\omega C_1+\frac{1}{Z_2}} + j\omega L_1 + r_1 \tag{12}$$

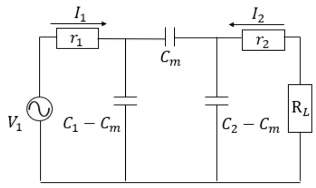

Fig 3 Non resonance(N-N)

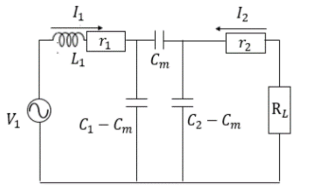

Fig 4 Primary resonance(S-N)

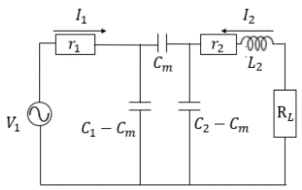

Fig 5 Secondary resonance(N-S)

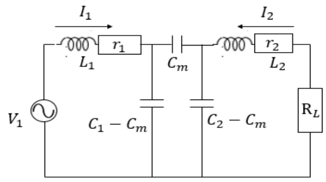

Fig 6 Electric resonant coupling(S-S)

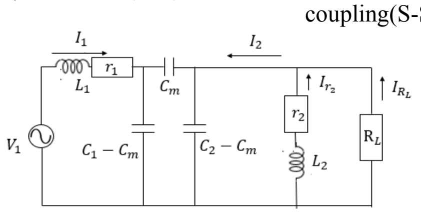

Fig 7 Electric resonant coupling(S-P)

Secondary resonance condition is satisfied when the imaginary part of the equation (10) becomes 0, so the equation of ω_2 is represented equation (13).

$$\omega_2 = \sqrt{\frac{1}{L_2C_2} - \left(\frac{R_L+r_2}{L_2}\right)^2} \tag{13}$$

Further, primary resonance condition is satisfied when the imaginary part of the equation (12) becomes 0, so the equation of ω_1 is represented equation (14).

$$\omega_1 = \sqrt{\frac{1}{L_1C_1} - \left(\frac{1}{C_1Z_2}\right)^2} \tag{14}$$

To derive efficiency, S-S loop current circuit is used in Fig.9.

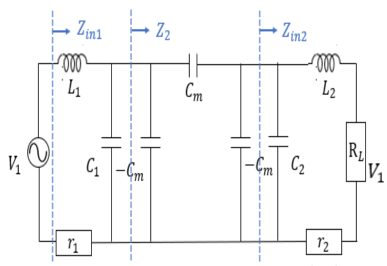

Fig 8 Expanded π-type equivalent

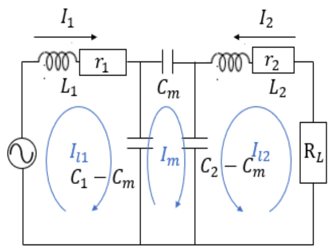

Fig 9 Loop current circuit(S-S)

From the circuit of Fig.9, the ratio of $|I_1|^2$ to $|I_2|^2$ can be expressed equation (15). Furthermore, from the equations (5) to (7), the ratio of the power consumption at each resistor can be expressed equation (16).

$$|I_1|^2 : |I_2|^2 = \omega^2 C_1C_2A + C_1^2(1-\omega^2L_2C_2) : C_m^2 \tag{15}$$

$$P_{r1} : P_{r_2} : P_{R_L} = r_1|I_1|^2 : r_2|I_2|^2 : R_L|I_2|^2$$
$$= r_1\{\omega^2(C_1C_2 - C_m^2)\{(C_1C_2 - C_m^2)A - L_2C_1\} + C_1^2\} :$$
$$r_2C_m^2 : R_LC_m^2 \tag{16}$$

$$\begin{cases} A = (R_L + r_2)^2 + (\omega L_2)^2 \\ B = {r_2}^2 + (\omega L_2)^2 \end{cases}$$

The efficiency equation is shown in equation (17) from equations (4) and (16). Further, taking the resonance condition (13) into account, the efficiency becomes the equation (18). Furthermore, the optimum load represent equation (20) from the equation (19).

$$\eta = \frac{R_LC_m^2}{r_1[C_1^2 + \omega^2(C_1C_2 - C_m^2)\{(C_1C_2 - C_m^2)A - 2L_2C_1\}] + (r_2 + R_L)C_m^2} \tag{17}$$

$$\eta = \frac{R_LL_2C_2^2C_m^2}{r_1\{C_2(R_L + r_2)^2(C_1^2C_2^2 - C_m^4) + L_2C_m^4\} + (r_2 + R_L)C_m^2C_2^2L_2} \tag{18}$$

$$\frac{d\eta}{dR_L} = 0 \tag{19}$$

$$R_{Lopt} = \sqrt{r_2^2 + \frac{L_2C_m^2(r_1C_m^2 + r_2C_2)}{r_1C_2(C_1^2C_2^2 - C_m^4)}} \tag{20}$$

Output power equation is derived. However, the output power equation is complicated, only the derivation method is shown. From (12), the input impedance can be expressed by (21). From (21), the output power can be expressed by (22)

$$Z_{in1} = R + jX \tag{21}$$

$$P_1 = \frac{R}{R^2+X^2}V_1^2 \tag{22}$$

In the same way, resonance conditions, efficiency, optimum load, and output power were derived in other topologies. Table.1 shows the equations of the primary and secondary resonance conditions.

Output power reaches the maximum value when the primary resonance condition is satisfied. And, efficiency reaches the maximum value when the secondary resonance condition is satisfied. So, secondary and primary resonance condition should be satisfied at optimum load so that high power and high efficiency transmission is realized. Then, primary resonance condition is satisfied by adjusting primary coil L_1, and secondary resonance condition is satisfied by adjusting primary coil L_2.

Next, derivation method of optimum load R_{Lopt}, primary resonance condition L_1 and secondary resonance condition L_2 is represented.

First, simultaneous equations of equation (13) and equation (20) is solved and, optimum load R_{Lopt} and secondary coil L_2 is derived. After that, primary coil L_1 is derived by substituting each value for equation (14). The actual values are shown in chapter 7.

Table 1 Resonance condition

	Primary resonance condition	Secondary resonance condition
S-N	$L_1=\frac{C_1+\omega^2C_2(r_2+R_L)^2(C_1C_2-C_m^2)}{\omega^2\{\omega^2(r_2+R_L)^2(C_1C_2-C_m^2)^2+C_1^2\}}$	
N-S		$\omega_2=\sqrt{\frac{1}{L_2C_2}-\left(\frac{R_L+r_2}{L_2}\right)^2}$
S-S	$L_1=\frac{C_1(R_L+r_2)^2-\omega^2\{C_2A-L_2\}\{C_1L_2-(C_1C_2-C_m^2)A\}}{\omega^4\{C_1L_2-(C_1C_2-C_m^2)A\}^2+\omega^2C_1^2(R_L+r_2)^2}$	$\omega_2=\sqrt{\frac{1}{L_2C_2}-\left(\frac{R_L+r_2}{L_2}\right)^2}$
S-P	$L_1=\frac{\{(R_Lr_2+B)^2+\omega^2R_L^2(L_2-C_2B)^2\}[C_1\{(R_Lr_2+B)^2+\omega^2R_L^2(L_2-C_2B)^2\}+\omega^2C_m^2R_L^2B(L_2-C_2B)]}{\omega^4C_m^4R_L^2B^2(R_Lr_2+B)^2+[\omega C_1\{(R_Lr_2+B)^2+\omega^2R_L^2(L_2-C_2B)^2\}+\omega^3C_m^2R_L^2B(L_2-C_2B)]^2}$	$\omega_2=\sqrt{\frac{1}{C_2L_2}-\left(\frac{r_2}{L_2}\right)^2}$

Table 2 Efficiency (any frequency)

	η
N-N	$\frac{R_LC_m^2}{r_1\{C_1^2+\omega^2(r_2+R_L)^2(C_1C_2-C_m^2)^2\}+(r_2+R_L)C_m^2}$
S-N	$\frac{R_LC_m^2}{r_1\{C_1^2+\omega^2(r_2+R_L)^2(C_1C_2-C_m^2)^2\}+(r_2+R_L)C_m^2}$
N-S	$\frac{R_LC_m^2}{r_1[C_1^2+\omega^2(C_1C_2-C_m^2)\{(C_1C_2-C_m^2)A-2L_2C_1\}]+(r_2+R_L)C_m^2}$
S-S	$\frac{R_LC_m^2}{r_1[C_1^2+\omega^2(C_1C_2-C_m^2)\{(C_1C_2-C_m^2)A-2L_2C_1\}]+(r_2+R_L)C_m^2}$
S-P	$\frac{R_LBC_m^2}{r_1\{\omega^2R_L^2(C_1C_2-C_m^2)\{B(C_1C_2-C_m^2)-2C_1L_2\}+C_1^2A\}+(B+r_2R_L)R_LC_m^2}$

Table 3 Efficiency (secondary side resonance)

	η
N-S	$\frac{R_LL_2C_2^2C_m^2}{r_1\{C_2(R_L+r_2)^2(C_1^2C_2^2-C_m^4)+L_2C_m^4\}+(r_2+R_L)C_m^2C_2^2L_2}$
S-S	$\frac{R_LL_2C_2^2C_m^2}{r_1\{C_2(R_L+r_2)^2(C_1^2C_2^2-C_m^4)+L_2C_m^4\}+(r_2+R_L)C_m^2C_2^2L_2}$
S-P	$\frac{R_LL_2^2C_2C_m^2}{r_1\{C_1^2C_2(C_2r_2R_L+L_2)^2+(L_2-C_2r_2^2)R_L^2C_m^4\}+(L_2+C_2r_2R_L)R_LC_m^2C_2L_2}$

Table 2 shows the efficiency equation at any frequency, and Table 3 shows the efficiency equation at the secondary side resonance. Table.4 shows the equation of optimum load at secondary side resonance.

Table 4 Optimum load at secondary side resonance

	$R_{L_{opt}}$
N-N	$\sqrt{r_2^2+\frac{r_1C_1^2+r_2C_m^2}{\omega^2r_1(C_1C_2-C_m^2)^2}}$
S-N	$\sqrt{r_2^2+\frac{r_1C_1^2+r_2C_m^2}{\omega^2r_1(C_1C_2-C_m^2)^2}}$
N-S	$\sqrt{r_2^2+\frac{L_2C_m^2(r_1C_m^2+r_2C_2^2)}{r_1C_2(C_1^2C_2^2-C_m^4)}}$
S-S	$\sqrt{r_2^2+\frac{L_2C_m^2(r_1C_m^2+r_2C_2^2)}{r_1C_2(C_1^2C_2^2-C_m^4)}}$
S-P	$L_2C_1\sqrt{\frac{r_1C_2}{r_1\{C_1^2C_2^3r_2^2+(L_2-C_2r_2^2)C_m^4\}+C_2^2C_m^2r_2L_2}}$

5. COMPARISON OF THEORETICAL FORMULA AND ANALYSIS

In this section, it is confirmed that the efficiency and output power equations match the curves analyzed by LTspice to show the validity of the equations.

Fig. 10 shows the relationship between efficiency and load in S-S under table.2 condition, and Fig. 11 shows the relationship between output power and frequency in S-S. The value of each element is shown in Table.5.

Table 5 The value of each element

	N-N	S-N	N-S	S-S	S-P
$f[Hz]$	450k	450k	450k	450k	450k
$C_1[F]$	390p	390p	390p	390p	390p
$C_2[F]$	410p	410p	410p	410p	410p
$C_m[F]$	40p	40p	40p	40p	40p
$L_1[H]$		320μ		320μ	320μ
$L_2[H]$			300μ	300μ	300μ
$r_1[\Omega]$	2.67	2.67	2.67	2.67	2.67
$r_2[\Omega]$	2	2	2	2	2
$v_1[V]$	100	100	100	100	100
$R_L[\Omega]$	100	100	100	100	100k
k	0.1	0.1	0.1	0.1	0.1

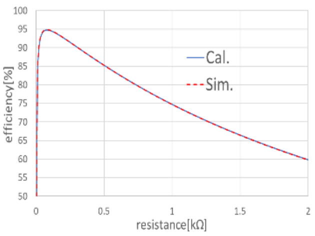

Fig 10 Inspection of efficiency

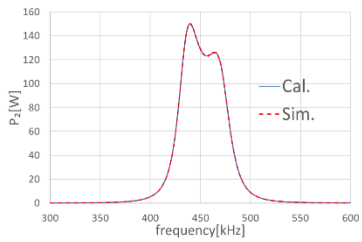

Fig 11 Inspection of power

As can be seen from Fig.10 and Fig.11, the theoretical and analytical curves are matched. From these results, it can be said that the efficiency and output power equations derived in the previous chapter is valid.

6. COMPARISON OF EFFICIENCY

Efficiency reaches the maximum value when the secondary resonance condition is satisfied. Therefore, efficiency researched when secondary resonance condition is satisfied.

That time, secondary resonance frequency changes. So, resonance frequency adjusted according to the change of load.

Figures 12 and 13 show the efficiency of each topology. Then, the value of each element is used the value of Table.5.

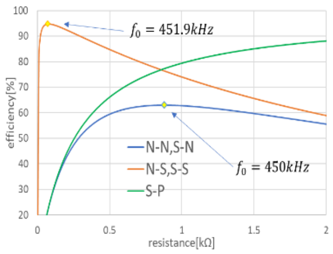

Fig 12 Efficiency (low load)

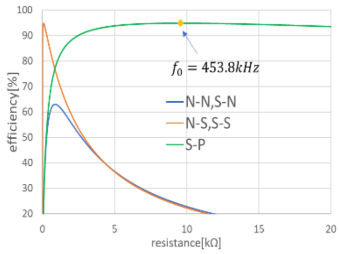

Fig.13 Efficiency (high load)

As can be seen from Fig.12 and Fig.13, N-S and S-S have excellent efficiency in low load area around 1 to 800Ω. Next to these, S-P has excellent efficiency in high load area. The yellow point is the point at the optimum load, and the resonance frequency at that time is shown on the graph.

-

7. CONDITIONS FOR HIGH-EFFICIENCY AND HIGH-POWER TRANSMISSION

In this section, the conditions for high-efficiency and high-power transfer are derived.

As described in Section 4, the optimum load in efficiency and the value of the resonance frequency are derived.

The optimum load in N-N and S-N is R_{Lopt}= 874.8 [Ω], the optimum load in N-S and S-S is R_{Lopt} = 76.4 [Ω], and the optimum load in S-P is R_{Lopt} = 9572.4 [Ω] from the equation of optimum load (Table.4). The same result can be seen from the graph in Fig.11.

Next, the resonance frequency at the optimum load was f_0= 451.9 [kHz] in N-S and S-S and f_0 = 453.8 [kHz] in S-P from the equation of secondary resonance condition (Table.1).

Next, resonance inductance L_1 is derived from equation of primary resonance condition (Table.1). In S-N, resonance inductance L_1 is adjusted so that primary resonance frequency becomes 450 [kHz].

Resonance inductance is L_1 = 322.4[μH] in S-N, L_1 = 321.3 [μH] in S-S, and L_1 = 315.4 [μH] in S-P

Figures 14 and 15 show the values of efficiency and load consumption power P_2 when power is transmitted with an optimum load based on the above results. $V_1 = 100[V]$.

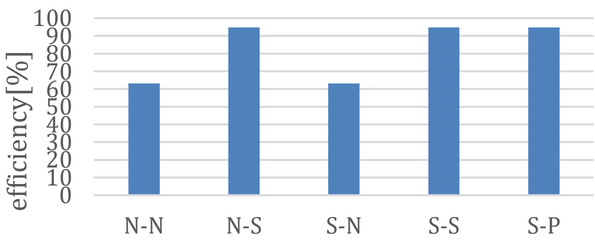

Fig 14 Efficiency of five different circuits

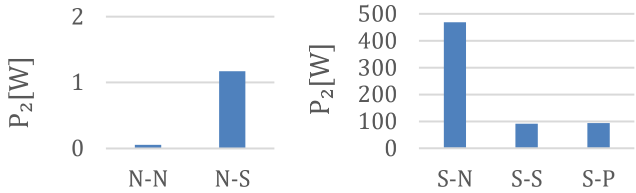

Fig 15 Consumed power of five different circuits

As shown in Fig. 14, N-N and S-N, the efficiency is only about 63% even at the optimum load, so it cannot be said that the efficiency is high. On the other hand, N-S, S-S, and S-P can transfer at an efficiency of nearly 95% at the optimum load. In addition, Fig.15 shows that S-S can transfer about 92W and S-P can transfer about 95W.

Therefore, S-S and S-P can transmit power with high efficiency and power. So, S-S and S-P are superior to other topologies.

8. CONCLUSION

In this paper, the five topologies: non-resonance (N-N), secondary resonance (N-S), primary resonance (S-N), electric resonant coupling (S-S) and (S-P) are compared by deriving equation of efficiency, optimum load, and output power.

Moreover, by selecting the primary side coil to the primary resonance condition, the value of efficiency and load consumption power are derived when optimum load and resonance condition is satisfied. As a result, it is said that S-S and S-P can transfer with high efficiency and high power and are superior to other topologies.

However, if it is enough that efficiency is beyond a certain level, there is a possibility that higher power transfer can be performed. So, it is necessary to continue to examine the efficiency and power of CPT. In the future, we would like to carry out comparison and inspection through experiment.

9. ACKNOWLEDFMENTS

This work was partly supported by JSPS KAKENHI Grant Number 17H04915

9. REFERENCES

[1]Aristeidis Kararis, et Al., “Wireless Power Transfer via Stronglk Coupled Magnetic Resonances”, Science Express,Vol.317,No.5834,pp.83-86,2007.

[2]Mitsuru MASUDA et ., “Wireless Power Transfer via Electric Field Resonance Coupling”, JIEP, Vol.18 No.5, 2015.

[3]Mitsuru MASUDA et ., “Wireless Power Transfer via Electric Coupling”, IEICE Technical Report , WPT2013-20

[4]Takashi OHIRA., “Via-Wheel Power Feed to Running Electric Vehicles” , IEICE Technical Report , WPT2012-17